Role of ERK activation in *H. pylori*-induced disruption of cell-cell tight junctions.

Amita Sekar[1,] and Bow Ho[1,2,]*

[1]Department of Microbiology and Immunology, National University of Singapore, Singapore 117545

[2]Department of Food Science & Technology, Faculty of Science, National University of Singapore 117546

*Corresponding author: E-mail: michob@gmail.com Phone: +65 65163092

Running title: *H. pylori*-induced tight junction disruption

Abstract

Background

Tight junctions, a network of claudins and other proteins, play an important role in maintaining barrier function and para-cellular permeability. *H. pylori*, the major etiological agent of various gastroduodenal diseases, is known to cause tight junction disruption. However, the molecular events that triggered cell-cell tight junction disruption in *H. pylori*-infected cells, remain largely elusive.

Materials and Methods

Trans-epithelial electrical resistance (TEER) and FITC-Dextran permeability measurement were performed to determine the barrier function in *H. pylori* 88-3887-infected polarized MKN28 cells. For visualization of tight junction protein localization, immunofluorescence and immunoblotting techniques were used. To examine the role of ERK activation in tight junction disruption, U0126, a MEK inhibitor, was employed. To further support the study,

computational analyses of *H. pylori*-infected primary gastric cells were carried out to decipher the transcriptomic changes.

Results

The epithelial barrier of polarized MKN28 cells when infected with *H. pylori* displayed disruption of cell-cell junctions as shown by TEER & FITC-dextran permeability tests. Claudin-4 was shown to delocalize from host cytoplasm to nucleus in *H. pylori*-infected cells. In contrast, delocalization of claudin-4 was minimized when ERK activation was inhibited. Interestingly, transcriptomic analyses revealed the upregulation of genes associated with cell-junction assembly and ERK pathway forming a dense interacting network of proteins.

Conclusion

Taken together, evidence from this study indicates that *H. pylori* regulates ERK pathway triggering cell-cell junction disruption, contributing to host pathogenesis. It indicates the vital role of ERK in regulating key events associated with the development of *H. pylori*-induced gastroduodenal diseases.

Introduction

Gastric mucosal barrier, which is composed of thick mucus layer and polarized epithelial cells, confers protection to the inner layers of the stomach from the hostile acidic environment[1][2]. Despite being a single layer of epithelial cells, it provides a sturdy wall against the highly corrosive contents of the gut, maintaining homeostasis. Polarized gastric epithelial cells harbour distinct domains of which the lateral domains comprise cell-cell junctions and account for establishing cell-cell contact and cell adhesion to the extracellular matrix[3]. Cell-cell tight junctions found at the apical side are responsible for the tight packaging of the cells and maintaining paracellular permeability. Tight junctions are

composed of transmembrane proteins such as Junction Adhesion Molecule (JAM), Occludins, Claudins and cytoplasmic connector protein Zona Occludens (ZO-1). Together, these proteins are closely associated to form a tight junction assembly[4] that maintain the cell barrier integrity.

Focussed research on claudins from the time of its discovery in 1998 has garnered mounting evidence that these junction proteins form the primary physical basis of tight junction assembly[5]. The homophilic and heterophilic interactions among different claudins as well as its association with the other components of tight junction complex is pivotal in ensuring proper functioning of the cell-cell tight junctions[6]. Till date, 27 claudins have been reported and they have been found in tissue specific combinations thereby conferring tissue-specific barrier properties[9]. Phosphorylation of claudins has been reported to play a vital role in paracellular permeability. Various kinases like myosin light chain kinase (MLCK) and protein kinase A (PKA) have been shown to be involved in the phosphorylation of claudins[10].

Kwon (2013) observed aberrant expression of cell-junction associated proteins in clinically isolated tumour samples[11]. Similarly, moderate to high staining of claudin-4 was correlated to decreased survival in gastric adenocarcinoma tissues suggesting a strong link between expression of tight junction proteins and cancer[12]. The altered expression and localization of another tight junction protein, ZO-1, was observed in metastatic pancreatic ductal adenocarcinoma tissue[13]. In contrast, reduced expression of several claudins has also been closely linked to tumorigenesis. Claudin-1 and -7 have been found to be deregulated in breast carcinoma while downregulation of claudin-4 was observed in hepatocellular carcinoma[9]. These studies highlight the importance of expression and localization of cell-junction protein in maintaining host cell integrity. Substantial evidence has thus led us to

consider cell junction proteins as potential biomarkers in various disease conditions, mostly in cancer.

Tight junction disruption has been reported to be caused by various microbes. In the course of pathogen infection, inflammation and other host responses have also shown to cause internalization of claudins which has a direct effect on the host cell homeostasis. Bacteria such as *Listeria monocytogenes*, *Campylobacter jejuni* and *Escherichia coli* have been shown to invade the host causing tight junction disruptions[14][15][16]. However, the mechanism by which these pathogens affect the cell-cell junction proteins to cause a physiological imbalance in host cells remains largely elusive.

Helicobacter pylori, an extensively studied gram negative gut pathogen has been highly associated with various gastro-duodenal diseases including gastric cancer[17][18]. More than half of the world's population are infected with this gut bacterium[19]. The bacterium harbors an array of virulence factors which aid in colonization of the gut. Bacterial proteins such as cytotoxin associated gene A (CagA) and vacuolating cytotoxin A (VacA) have been determined to be of high importance in *H. pylori* pathogenesis[20]. *H. pylori* has been reported to translocate CagA via the type IV secretion system (T4SS) into the host cells triggering events such as IL-8 induction, cytoskeletal rearrangement and many other host responses[21][22]. Intriguingly, the CagA-T4SS system was found to interact with basolateral integrins to translocate the virulence factor into the host[23][24]. These findings have led to speculate that *H. pylori* could induce cell-cell junction disruption prior to accessing the basolateral integrins in order to translocate CagA into the host[25]. In 2003, Ameiva *et al* observed that CagA could play a role in recruiting ZO-1 to the sites of bacterial attachment and cause cytoskeletal rearrangement[26]. Factors such as high temperature requirement A (HtrA) have been reported to aid in *H. pylori*–induced cell junction disruption[27]. In other studies, *H. pylori* urease has been implicated in causing tight junction disruption by targeting

claudin-4 and -5[28][29]. Even though strong evidence suggests the involvement of *H. pylori* in tight junction disruption, the exact mechanism by which the bacterium induces tight junction disruption remains unclear.

ERK is a major transcription factor involved in the expression of many crucial proteins determining the fate of host cell. *H. pylori* has been shown to activate ERK triggering many host response pathways[30][31][32][33][34]. Several reports have strongly implicated the role of activated ERK in regulating cell junction proteins, particularly claudins, and in disrupting cell-cell barrier function. Wang *et al*., (2004) demonstrated that activation of ERK1/2-MAPK pathway was found to disrupt tight junctions in human corneal epithelial cells[35]. Interestingly, Aggarwal *et al* in 2011 reported that knockdown of ERK1/2 enhanced tight junction integrity while U0126 (ERK kinase inhibitor) attenuated the disruption initiated by the activation of EGFR[36]. In contrast, Ray *et al* in 2007 revealed that MEK1/ERK is highly associated with maintaining cell-cell contacts[37]. A recent published study observed that inhibition of ERK signaling pathway decreased the expression of claudin-2 in lung adenocarcinoma cells[38] and similar results were also observed in Madin-Darby Canine Kidney cells (MDCK) I and II cells[39]. Although several studies have explored the role of *H. pylori*-induced ERK activation, there is a knowledge gap regarding its effect on tight junction proteins and barrier function disruption.

Our study aims to deduce the role of ERK activation in *H. pylori*-induced barrier function disruption. We present data showing the role of *H. pylori*-induced ERK activation in delocalizing claudin-4 from the tight junctions leading to the disruption of barrier function in MKN28 cells. This study also provides supporting data from transcriptomic analysis of *H. pylori*-infected primary cells showing significant regulation of tight junction and ERK signalling related gene expression.

Methods

Bacterial and in vitro cell cultures

H. pylori 88-3887 strain was used in this study. Bacteria were grown in 5% chocolate blood agar plates at 37˚C in a 10% CO_2 incubator (Forma Scientific, USA) for two days before being harvested and suspended in phosphate buffered saline (PBS). A standard curve was generated based on the correlationship between the optical density readings of bacterial suspensions and bacterial count using plate count.

Polarized MKN28 cells were used as the study model as these cells have been shown to form intact cell-cell junctions[29]. The cells were cultured and maintained in RPMI 1640 with 2.05 mM L-glutamine (HyClone, USA) supplemented with 10% Fetal Bovine Serum (HyClone, USA) and incubated at 37˚C in a 5% CO_2 incubator (Forma Scientific, USA). The polarized cells were grown to above 90% confluency to ensure formation of intact cell junctions.

Materials

FITC-Dextran- 4kDa used in permeability assay was purchased from Sigma-Aldrich, USA. Mouse monoclonal anti-Claudin-4 (1:100, Novex, Life Technologies, USA) and rabbit polyclonal anti-claudin-4 (1:1000, Santa Cruz Biotechnology, USA) were used in immunofluorescence and immunoblotting experiments respectively. Rabbit polyclonal anti-*H. pylori* (1:250) was from Dako, Denmark and mouse monoclonal anti- *H. pylori* (1:250) was from Thermo Scientific, USA. Mouse monoclonal Beta-actin (1:3000) from Cell Signalling Technologies, USA was used as marker for whole cell protein immunoblotting experiments. Rabbit polyclonal p-cadherin (1:1000, Santa Cruz Biotechnology, USA), Rabbit polyclonal beta-tubulin (1:1000, Cell Signalling Technologies, USA) and Rabbit polyclonal anti-Lamin A/C (1:1000, Cell Signalling Technologies, USA) were used as markers for

membrane, cytoplasmic and nuclear protein respectively. ERK activation was assessed using rabbit polyclonal anti-p-ERK (1:500, Cell Signalling Technologies, USA). Polyclonal goat anti-mouse IgG/HRP and Polyclonal goat anti-rabbit IgG/HRP (1:2000) were from Dako, Denmark. Fluorescent conjugated secondary antibodies Cy3 goat anti-mouse IgG (H+L) (1:100), Cy3 goat anti-rabbit IgG (H+L) (1:100), Alexafluor 488 F(ab')2 fragment of goat anti-rabbit IgG (H+L) (1:100) and Alexafluor 488 goat anti-mouse IgG (H+L) (1:100) were all purchased from ThermoFisher Scientific, USA. U0126 (MEK inhibitor) was purchased from Cell Signaling Technologies, USA. For the inhibitor study, the cells were treated with 10uM U0126 (Tocris Biosciences, UK).

Infection study

The confluent cells were infected with *H. pylori* 88-3887 at a multiplicity of infection (MOI) of 100:1. The cells were then incubated at 37˚C in a 5% CO_2 incubator for 24 hrs or various time points as required for the experiment. Post infection, the cells were washed 3 times with 1x PBS prior to any further downstream processing.

Immunofluorescence studies

Cells were cultured on sterilized coverslips placed in 6-well plates (Greiner Bio-One, Austria) containing culture medium RPMI 1640 for 3-4 days. The confluent cells were treated with inhibitor and/or infected with *H. pylori* while uninfected cells served as control. At the required time points, the cover slips containing the cells were withdrawn and washed twice with 1 x PBS before being fixed using 3.7% formaldehyde. Following this, the cells were permeabilized using 3.7% formaldehyde and 0.02% Triton X-100 (Sigma-Aldrich, USA). Blocking was carried out with 2% Bovine Serum Albumin (BSA) (Sigma-Aldrich, USA) for 2 hours, prior to incubating with primary antibodies at 4˚C overnight. The cells were then washed thrice with 1 x PBS for 5 mins each prior to incubating with fluorescent

conjugated secondary antibodies for 2 hours at room temperature. The coverslips containing the immuno-stained cells were washed thrice with 1 x PBS then mounted onto glass slides using mounting media with DAPI (Vector Laboratories, Inc., USA). The stained cells were viewed using confocal laser scanning microscopy (CLSM) (Olympus FV3000, Japan).

3D image reconstruction: z-stack images were taken using CLSM and these images were loaded onto Imaris software (version 7.6, Bitplane) for reconstructing the images in a 3D plane. These images were used to analyse the delocalization of claudin-4 from the apical membrane.

Transepithelial electrical resistance (TEER) measurement

Cells were cultured in 12-well plate hanging inserts (Greiner Bio-One, Austria) for 3-4 days to reach > 90% confluency. TEER readings were measured using the electrode supplied along with the MilliCell-ERS volt-ohm meter (Merck, USA). A blank insert with media alone was used as a negative control. MKN28 cells with TEER reading > 350 $\Omega.cm^2$ was considered optimal for the barrier function studies. TEER readings were measured for cells subjected to inhibitor treatment and/or infected with *H. pylori*. Uninfected cells served as control. The % baseline resistance was calculated using the following equation and the values were plotted as a graph. All experiments were performed in triplicates.

$$\% \text{ Baseline Resistance} = \frac{[\text{Sample Resistance} - \text{Blank Resistance}]}{[\text{Baseline Resistance} - \text{Blank Resistance}]} \times 100$$

FITC-Dextran permeability assay

MKN28 cells were cultured for 3-4 days to confluency in 12-well inserts and subjected to inhibitor treatment and/or infection with *H. pylori*. Uninfected cells served as control. The cells were washed twice with 1 x PBS before adding FITC-Dextran (1mg/ml) to

188 the upper chamber. The FITC-Dextran that diffused into the basal chamber media was
189 determined by measuring the fluorescence intensity at optical density 492nm (Tecan Infinite,
190 Switzerland). All experiments were performed in triplicates.

191 *Protein extraction and western blot studies*

192 Post infection cells were lysed using Triton-X 100 containing lysis buffer to extract
193 whole cell proteins. Membrane and cytoplasmic protein fractions of cells infected with *H.*
194 *pylori* for 24 hours were extracted using ProteoJet™ Membrane Protein extraction kit
195 (Fermentas, Thermo Scientific, USA) according to the manufacturer's protocol. Cytoplasmic
196 and nuclear fractions were separated using NE-PER™ Nuclear and Cytoplasmic Extraction
197 Reagents (Thermo Scientific, USA). The protein concentration of samples were estimated
198 using Bradford Assay (Bio Rad, USA) and an equivalent of 15ug protein was loaded onto
199 12% SDS- Poly Acrylamide gel and subjected to protein electrophoresis. The samples were
200 then electro-blotted onto PVDF membrane by wet transfer method. The membranes were
201 blocked with 2% BSA prior to incubating with primary antibodies at 4˚C overnight. The
202 membranes were then washed thoroughly with 1xPBS with 0.1% Tween- 20 (Sigma-Aldrich,
203 USA) for 5 times of 5 mins each. The membranes were then incubated with HRP-conjugated
204 secondary antibodies for 2 hours at room temperature. After thorough washing (5 x 5 mins),
205 the membranes were developed using Pierce ECL western blotting substrate (Thermo
206 Scientific, USA) and the bands were documented using ChemiDoc™ MP System (Bio-Rad
207 Laboratories, USA).

208 *q-PCR studies*

209 RNA was extracted from infected and uninfected cells using RNeasy Mini kit
210 (Qiagen, USA) and quantitated spectrophotometrically. Specific primers for claudin-4
211 [Forward primer 5'-TGGGAGGGCTATGGATGAA-3', Reverse Primer 5'-

GCTTTCATCCTCCAGGCAGT-3'] and endogenous control GAPDH [Forward primer 5'-ATCTCCCCTCCTCACAGTTG-3', Reverse Primer 5'-TGGTTGAGCACAGGGTACTT-3'] were synthesized by Sigma-Aldrich, USA. These primers were used to amplify the mRNA from the sample using Quantifast SyBR Green one –step RT-PCR kit (Qiagen, Netherlands) and the reactions were run using ABI 7500 real-time PCR instrument (Thermo Scientific, USA). The experiment was performed in triplicates and the relative quantitation values were analysed using 7500 software v2.0.6 (Thermo Scientific, USA) and represented as a graph.

Bioinformatic analysis

Published RNA-Seq raw data of *H. pylori*-infected gastric primary cells were used for downstream analysis (Accession number: GSE55699)[40]. The published libraries were downloaded from Gene Expression Omnibus[41].

The fastq format raw reads were subjected to quality control analysis using FASTQC (http://www.bioinformatics.babraham.ac.uk/projects/fastqc/). The sequencing files were considered to be of high quality when the following parameters were observed: (Mean Quality score-30 and above, Adapter contamination level- Below 0.01%, Duplication level-Below 80%, %A ~%T, %G~%C).

Mapping of the RNA-Seq libraries was performed using the splicing-aware STAR 2.4. The software ensured trimming of unmappable and low quality sequences. Reads with more than 2 mismatches and reads that map to more than one locus in the genome were filtered out. The mapped files were imported into SeqMonk 0.31.0 (http://www.bioinformatics.babraham.ac.uk/projects/seqmonk/) and the replicates and sample groups were assigned appropriately. Mapping QC was performed using "RNA-Seq QC Plot" option. Differential gene expression analysis was carried out using the in-built EdgeR

statistics module[42]. Mapped files were then normalized using the log10 (RPKM) transformation option in RNA-Seq quantitation pipeline module. Heatmaps of the significant genes were generated using the "Per-probe normalized Hierarchical Clustering" option. Gene Ontology terms file (.bgo) and the human gene ontology annotation file were downloaded from the gene ontology consortium website (http://geneontology.org/). These files were imported to BiNGO[43] application which is installed in Cytoscape 3.2.0[44]. List of significant genes was uploaded to BiNGO to identify the enriched biological processes. Gene lists of relevant biological processes were uploaded to STRING (http://string-db.org/) protein-protein interaction database[45]. The text mining option was disabled. The interaction network was downloaded in text format. The text file was uploaded to Cytoscape 3.2.0 for visualization.

Statistical analysis

Student t-test (2-tailed, paired end) was used to calculate the p-value and determine statistical significance.

Results

H. pylori affects barrier function and impairs the localization of claudin-4 in MKN28 cells.

Cell-cell junctions confer epithelial barrier function and play a critical role in permeability. Epithelial barrier function of polarized MKN28 cells were determined using Trans-epithelial electrical resistance (TEER) measurement and FITC-Dextran permeability assay. TEER readings taken 24 hours post-*H. pylori* infection were found to be significantly reduced (p-value = 0.009050856) in *H. pylori*-infected cells when compared to the uninfected control (Fig. 1A, left panel). Similarly, permeability of 4kDa FITC-Dextran was found to be higher in *H. pylori*-infected cells compared to uninfected cells (Fig. 1A, right panel). The

study demonstrates *H. pylori*-induced barrier function disruption in *H. pylori*-infected MKN28 cells using these two techniques.

In order to visualize the localization of claudin-4 in *H. pylori*-infected and uninfected cells, confocal laser scanning microscopy (CLSM) imaging was used. Within 24 hours of apical exposure of MKN28 cells to *H. pylori*, delocalization of claudin-4 from the cell-cell tight junctions was observed when compared to uninfected cells. Fig. 1B shows 3D reconstruction of the z-stack images of both *H. pylori*-infected and uninfected cells. The 3D images clearly display delocalization of claudin-4 from the tight junctions. *H. pylori*-infected cells showed cytoplasmic and peri-nuclear staining of claudin-4 whereas the uninfected cells showed localization of these proteins at the cell-cell junctions marking clear boundaries between cells (Fig. 1B).

To further support the finding that *H. pylori* affects the localization of claudin-4, western blot analysis was employed to examine the expression of claudin-4 in the membrane, cytoplasmic and nuclear protein fractions. The result shows an increased cytoplasmic and nuclear expression of claudin-4 suggesting delocalization of these proteins from cell-cell junction in *H. pylori*-infected cells. Furthermore, the membrane claudin-4 expression in *H. pylori*-infected cells was found to be reduced when compared to uninfected cells affirming the delocalization of claudin-4 (Fig. 1C).

We next examined the overall protein and mRNA expression of claudin-4 of uninfected cells and *H. pylori*-infected cells using western blot analysis and qPCR studies. We found that the protein expression did not differ between *H. pylori*-infected cells and uninfected cells at various time points studied (Fig. 1D, upper panel). Similarly, mRNA expression of claudin-4 in *H. pylori*-infected and uninfected cells did not differ (Fig. 1D,

lower panel). The results indicate that *H. pylori* induced delocalization of claudin-4 is not dependant on the expression level.

Inhibition of ERK activation minimized H. pylori-induced delocalization of claudin-4

It was reported that during *H. pylori* infection, increased levels of EGF-related peptides and NOD1 dependant mechanisms activate ERK[34]. Wang *et al* in 2004 demonstrated that ERK activation triggered barrier function disruption in human corneal epithelial cells[35]. We therefore proceeded to investigate whether inhibition of ERK activation using MEK inhibitor (U0126) would alter the process of *H. pylori*-induced barrier function disruption. Results show increased epithelial resistance (TEER) was detected in U0126-treated *H. pylori*-infected cells as compared to infected cells without inhibitor treatment (p-value = 0.003098682) (Fig. 2A, left panel). Interestingly, uninfected cells with or without inhibitor treatment showed similar TEER values. Furthermore, there was reduced permeability of 4kDa FITC-Dextran in *H. pylori*-infected cells with U0126 treatment as compared to infected cells without inhibitor treatment (Fig. 2A, right panel). The results show that upon the inhibition of *H. pylori*-induced ERK activation, the host epithelial barrier function is normalized. The data suggest that *H. pylori*-induced ERK activation has an important role in regulating epithelial barrier function in MKN28 cells supporting the findings of Wang et al (2004) demonstrated in corneal epithelial cells[35].

CLSM was used to further investigate the role of *H. pylori*–activated ERK in delocalizing claudin-4 in support of the TEER and FITC-Dextran results. Immuno staining of *H. pylori*-infected MKN28 cells treated with ERK activation inhibitor (U0126) showed minimized redistribution of claudin-4 when compared with *H. pylori*-infected cells without inhibitor treatment (Fig. 2B). More interestingly, western blots demonstrated that the

redistribution of claudin-4 from membrane to cytoplasm and nucleus was clearly reduced in U0126-treated *H. pylori*-infected cells (Fig.2C).

Transcriptomic changes induced by H. pylori infection leads to cell junction disruption

Our findings have thus demonstrated that *H. pylori* (infection?) plays an essential role in the disruption of epithelial barrier function with the involvement of ERK activation. In order to further elucidate the role of *H. pylori* in regulating signalling pathways and induce cell-cell junction disruption, RNA-Seq analysis was performed on *H. pylori*-infected primary gastric epithelial cells.

In this study, quality control analysis of the downloaded libraries was executed and the output showed that the mean quality score of the reads is ~37 indicating high quality sequencing[40]. Following which, mapping of the raw reads was accomplished. The percentage of uniquely mapped reads was ~92% with over 90% of those reads mapped to exons. This indicates the reliability of the libraries for further downstream analyses. Subsequently, differential gene expression analysis revealed that 8472 genes were significantly regulated in *H. pylori*-infected cells. Of these, 3665 genes were found to be upregulated while 4807 were downregulated (Fig. 3A). Further to this, the differential regulated genes as shown in Fig. 3B, were found to include interleukin-8 (IL8) and matrix metalloproteinase 10 (MMP10). These two genes have previously been shown to be upregulated in response to *H. pylori* infection[46][47] further supporting the credibility of the differential gene expression analysis. The scatter plot also shows the upregulation of the genes that are associated with tight junction assembly and host signalling pathway (CLDN18, MAP2K1 and NFKB1A) (Fig. 3B).

The scaled Reads Per Kilobase Million (RPKM) values of all the significantly regulated genes were visualized across the replicates using a hierarchical clustered heatmap.

Among the significantly upregulated genes (cutoff p-value = <0.05), we found many genes which are closely associated with tight junction assembly as well as MAPK cascade indicating that both the processes are heavily affected in *H. pylori*-infected cells. The heatmap also demonstrated similar expression profile among the replicates of each condition (Fig. 3C). Additionally, gene ontology analysis of *H. pylori* upregulated genes shows enrichment of cell junction assembly and MAPK cascade regulation processes. This has provided more evidence suggesting the role of *H. pylori* in the regulation of these two processes. Other processes such as response to bacterial proteins and inflammation were also observed to be enriched (Fig. 3D).

The upregulated genes associated with cell junction assembly and MAPK cascade were further subjected to protein-protein interaction analysis using STRING database and visualized using Cytoscape 3.2.0. Most astoundingly, the network reveals a strong protein-protein interaction among the upregulated genes involved in both the indicated biological processes forming an extremely tight network (Fig. 3.E). This result highly suggests the extent of gene regulation exerted by *H. pylori* on host cells where the bacterium induces disruption of cell-cell junction disruption via activation of MAPK/ERK associated pathways.

Discussion

Cell-cell tight junctions, being at the apical surface, constitute an important protective barrier which when compromised can lead to a multitude of deleterious effects on the host. Thus, the proteins that are responsible for forming the tight junction assembly could be crucial targets for pathogens to initiate pathogenesis. Claudins, one of the two major tight junction protein complex, are highly expressed in gastric tissue and has been shown to have aberrant expression and localization in cancer conditions[48]. It has also been reported to be a multifunctional protein with many roles in cell migration, cell signalling and barrier

maintenance[49]. In the event of infection and inflammation, internalization of claudins could lead to deleterious effects on the cell[8]. A recent study has shown that claudin-4 was over-expressed in 71% of 192 gastric cancer cases studied[50]. The importance of claudin-4 in normal function of gastric mucosal barrier should not be overlooked. Our study examines the course of claudins (in particular claudin-4) during *H. pylori* infection.

In this study, polarized MKN28 cells were used thanks to the organized cell–cell junctions[29]. The deleterious effect of *H. pylori* on disrupting the barrier function of MKN28 cells was shown by, the significant reduction in the TEER measurements and a concomitant increase in FITC-Dextran permeability in *H. pylori*- infected cells. Our findings strongly suggest that *H. pylori* induces delocalization of claudin-4 via activated ERK pathway leading to the loss of barrier function of the cell-cell tight junctions. The results support earlier reports that *H. pylori* impairs barrier function during pathogenesis[29][51][52].

Our initial data suggest that claudin-4 is redistributed from the cell-cell tight junctions into the cytoplasm. This is in agreement with several earlier reports that suggested the delocalization of tight junction proteins as a marker for transformed cells[9][11]. But, Fedwick *et al*., (2005) reported that *H. pylori* SS1-infected non-transformed polarized SCBN cells showed both the disruption of cell-cell junction and the reduction of the total protein level of claudin-4 and -5[28]. In order to visualize the effect of *H. pylori* on host claudin-4, we used immunofluorescence imaging which clearly show the delocalization of claudin-4 from cell-cell tight junctions to the cytoplasm and nucleus in *H. pylori*-infected cells. Furthermore, there was no obvious display of diminished staining-density of claudin-4 (Fig. 1B). Our confocal finding is further supported by western blot analysis and qPCR data (Fig. 1D) that revealed the overall level of expression of claudin-4 did not alter. Furthermore, western blot analysis (Fig. 1C) showed an increase of claudin-4, an apically expressed protein, in the cytoplasmic fraction but a decrease in the membrane fraction in *H. pylori*-infected cells.

Additionally, the expression of claudin-4 in the nuclear fraction was also found to increase in *H. pylori*-infected cells as compared to uninfected cells. Taken together, the findings in this study affirm that there is delocalization but not reduction in claudins in *H. pylori*-infected cells as reported earlier [28][53].

Activated ERK pathway has been reported to play a major role in inducing various host responses during pathogenesis[33][34]. Studies have reported that during *H. pylori* infection, increased levels of EGF and other related proteins have been shown to activate the EGFR pathway, signalling a cascade of events thereafter[54]. Of interest are recent reports that suggested activated ERK molecules have a role in epithelial barrier dysfunction[35][55]. By inhibiting ERK activation using U0126 in *H. pylori*-infected cells, there was significant reduction in the delocalization of claudin-4 (Fig.2B). Similarly, redistribution of claudin-4 into the cytoplasmic and nuclear region was reduced as compared to *H. pylori*-infected cells treated with U0126 (Fig.2C). Furthermore, the cell-cell barrier function in MKN28 cells was found to be maintained in cells treated with U0126 prior to infection (Fig.2A). It is therefore opportune to implicate that the activated ERK plays a role in delocalizing claudin-4 as a host response to *H. pylori* infection.

Our computational analysis demonstrated that *H. pylori* triggers the differential expression of many crucial genes including IL8 and MMP10 (Fig.3B) which is in agreement with the earlier reports that indicated these genes were regulated by *H. pylori*[46][47]. In addition to that, our RNA-Seq analysis revealed the upregulation of a large number of genes associated with MAPK cascade (Fig.3C). This is congruent with an earlier report that demonstrated the activation of MAPK cascade in *H. pylori*-infected cells, in a dose dependent manner[56]. However, our study is the first to report the extent by which *H. pylori* regulates the genes associated with the activation of MAPK cascade and cell junction assembly. Interactome analysis reveals that the upregulated MAPK cascade and cell junction genes

403 interact closely with each other forming a tight and strong network (Fig. 3E). This asserts that
404 the regulation of cell junction assembly by *H. pylori* could potentially be associated to the
405 activation of MAPK cascade. This study reveals for the first time that *H. pylori*-activated
406 ERK/MAPK cascade plays a significant role in disrupting cell-cell junctions in gastric
407 epithelial cells.

408 This study has provided evidence suggesting *H. pylori*-activated ERK pathway plays
409 a direct role in redistributing claudin-4 from the tight junctions resulting in compromising
410 host barrier integrity. Interestingly, the transcriptomic analyses also revealed a wealth of
411 information on the strong interactions at the molecular level between tight junction proteins
412 and ERK signalling proteins. However, further analyses involving the genome binding
413 occupancy profiling of transcription factors that are upregulated in *H. pylori*- infected cells
414 are required to decipher the molecular mechanism by which *H. pylori* causes tight junction
415 disruption via ERK activation.

416

417 **Conflict of interest**

418 Authors declare no conflict of interest.

419 **References**

420 1. Forssell H. Gastric mucosal defence mechanisms: a brief review. *Scand J*
421 *Gastroenterol Suppl* .1988;155:23-28.

422 2. Niv Y, Banić M. Gastric barrier function and toxic damage. *Dig Dis*. 2014;32:235-
423 242.

3. Chiba H, Osanai M, Murata M, Kojima T, Sawada N. Transmembrane proteins of tight junctions. *Biochim Biophys Acta*. 2008; 1778: 588-600.

4. Ebnet K. Organization of multiprotein complexes at cell-cell junctions. *Histochem Cell Biol*. 2008;130:1-20.

5. Tsukita S, Furuse M. Occludin and claudins in tight-junction strands: leading or supporting players? *Trends Cell Biol*. 1999;9:268-273.

6. Krause G, Protze J, Piontek J. Assembly and function of claudins: Structure-function relationships based on homology models and crystal structures. *Semin Cell Dev Biol*. 2015;42:3-12.

7. Veshnyakova A, Protze J, Rossa J, Blasig IE, Krause G, Piontek J On the interaction of Clostridium perfringens enterotoxin with claudins. *Toxins (Basel)*. 2010;2:1336-1356.

8. Findley MK, Koval M. Regulation and roles for claudin-family tight junction proteins. *IUBMB Life*. 2009;61:431-437.

9. Tsukita S, Tanaka H, Tamura A. The claudins: from tight junctions to biological systems. *Trends Biochem Sci*. 2019;44:141-152.

10. Shen L, Black ED, Witkowski ED, et al. Myosin light chain phosphorylation regulates barrier function by remodeling tight junction structure. *J Cell Sci* 2006;119:2095-2106.

11. Kwon MJ. Emerging roles of claudins in human cancer. *Int J Mol Sci* 2013;14:18148-18180.

12. Resnick MB, Gavilanez M, Newton E, et al. Claudin expression in gastric adenocarcinomas: a tissue microarray study with prognostic correlation. *Hum Pathol.* 2005;36:886-892.

13. Kleeff J, Shi X, Bode HP, et al. Altered expression and localization of the tight junction protein ZO-1 in primary and metastatic pancreatic cancer. *Pancreas.* 2001;23:259-265.

14. Hanajima-Ozawa M, Matsuzawa T, Fukui A, et al. Enteropathogenic *Escherichia coli*, *Shigella flexneri*, and *Listeria monocytogenes* recruit a junctional protein, zonula occludens-1, to actin tails and pedestals. *Infect Immun.* 2007;75:565-573.

15. Lamb-Rosteski JM, Kalischuk LD, Inglis GD, Buret AG. Epidermal growth factor inhibits Campylobacter jejuni-induced claudin-4 disruption, loss of epithelial barrier function, and Escherichia coli translocation. *Infect Immun.* 2008;76:3390-3398.

16. Zhang Q, Li Q, Wang C, Li N, Li J. Redistribution of tight junction proteins during EPEC infection in vivo. *Inflammation.* 2012;35,23-32.

17. Graham DY. History of *Helicobacter pylori*, duodenal ulcer, gastric ulcer and gastric cancer. *World J Gastroenterol.* 2014;20:5191-5204.

18. Sokic-Milutinovic A, Alempijevic T, Milosavljevic T. Role of *Helicobacter pylori* infection in gastric carcinogenesis: Current knowledge and future directions. *World J Gastroenterol.* 2015;21:11654-11672.

19. Kusters JG, van Vliet AH, Kuipers EJ. Pathogenesis of *Helicobacter pylori* infection. *Clin Microbiol Rev.* 2006;19:449-490.

20. da Costa DM, Pereira Edos S, Rabenhorst SH. What exists beyond cagA and vacA? *Helicobacter pylori* genes in gastric diseases. *World J Gastroenterol.* 2015;21:10563-10572.

21. Backert S, Ziska E, Brinkmann V, et al. Translocation of the *Helicobacter pylori* CagA protein in gastric epithelial cells by a type IV secretion apparatus. *Cell Microbiol.* 2000;2:155-164.

22. Hatakeyama M. SagA of CagA in *Helicobacter pylori* pathogenesis. *Curr Opin Microbiol.* 2008;11:30-37.

23. Kwok T, Zabler D, Urman S, et al. Helicobacter exploits integrin for type IV secretion and kinase activation. *Nature*. 2007;449:862-866.

24. Jiménez-Soto LF, Kutter S, Sewald X, et al. *Helicobacter pylori* type IV secretion apparatus exploits beta1 integrin in a novel RGD-independent manner. *PLoS Pathog.* 2009;5:e1000684.

25. Wessler S, Backert S. Molecular mechanisms of epithelial-barrier disruption by *Helicobacter pylori*. *Trends Microbiol.* 2008;16:397-405.

26. Amieva MR, Vogelmann R, Covacci A, Tompkins LS, Nelson WJ, Falkow S. Disruption of the epithelial apical-junctional complex by *Helicobacter pylori* CagA. *Science.* 2003;300:1430-1434.

27. Hoy B, Löwer M, Weydig C, et al. *Helicobacter pylori* HtrA is a new secreted virulence factor that cleaves E-cadherin to disrupt intercellular adhesion. *EMBO Rep.* 2010; 11:798-804.

28. Fedwick JP, Lapointe TK, Meddings JB, Sherman PM, Buret AG. *Helicobacter pylori* activates myosin light-chain kinase to disrupt claudin-4 and claudin-5 and increase epithelial permeability. *Infect Immun.* 2005;73:7844-7852.

29. Caron TJ, Scott KE, Fox JG, Hagen SJ. Tight junction disruption: *Helicobacter pylori* and dysregulation of the gastric mucosal barrier. *World J Gastroenterol.* 2015;21:11411-11427.

30. Meyer-ter-Vehn T, Covacci A, Kist M, Pahl HL. *Helicobacter pylori* activates mitogen-activated protein kinase cascades and induces expression of the proto-oncogenes c-fos and c-jun. *J Biol Chem.* 2000;275:16064-16072.

31. Subhash VV, Ho B. Inflammation and proliferation - a causal event of host response to *Helicobacter pylori* infection. *Microbiology.* 2015;161:1150-1160.

32. Asim M, Chaturvedi R, Hoge S, et al. *Helicobacter pylori* induces ERK-dependent formation of a phospho-c-Fos c-Jun activator protein-1 complex that causes apoptosis in macrophages. *J Biol Chem.* 2010;285:20343-20357.

33. Seo JH, Lim JW, Kim H. Differential Role of ERK and p38 on NF- κ B Activation in *Helicobacter pylori*-Infected Gastric Epithelial Cells. *J Cancer Prev.* 2013;18:346-350.

34. Allison CC, Kufer TA, Kremmer E, Kaparakis M, Ferrero RL. *Helicobacter pylori* induces MAPK phosphorylation and AP-1 activation via a NOD1-dependent mechanism. *J Immunol.* 2009;183:8099-8109.

35. Wang Y, Zhang J, Yi XJ, Yu FS. Activation of ERK1/2 MAP kinase pathway induces tight junction disruption in human corneal epithelial cells. *Exp Eye Res.* 2004;78:125-136.

512 36. Aggarwal S, Suzuki T, Taylor WL, Bhargava A, Rao RK. Contrasting effects of ERK
513 on tight junction integrity in differentiated and under-differentiated Caco-2 cell
514 monolayers. *Biochem J*. 2011;433:51-63.

515 37. Ray RM, Vaidya RJ, Johnson LR. MEK/ERK regulates adherens junctions and
516 migration through Rac1. *Cell Motil Cytoskeleton.* 2007;64:143-156.

517 38. Ikari A, Sato T, Watanabe R, Yamazaki Y, Sugatani J. Increase in claudin-2
518 expression by an EGFR/MEK/ERK/c-Fos pathway in lung adenocarcinoma A549
519 cells. *Biochim Biophys Acta.* 2012;1823:1110-1118.

520 39. Lipschutz JH, Li S, Arisco A, Balkovetz DF. Extracellular signal-regulated kinases
521 1/2 control claudin-2 expression in Madin-Darby canine kidney strain I and II cells. *J*
522 *Biol Chem*. 2005;280:3780-3788.

523 40. Koeppel M, Garcia-Alcalde F, Glowinski F, Schlaermann P, Meyer TF. *Helicobacter*
524 *pylori* infection causes characteristic DNA damage patterns in human cells. *Cell Rep.*
525 2015;11:1703-1713.

526 41. Edgar R, Domrachev M, Lash AE. Gene Expression Omnibus: NCBI gene expression
527 and hybridization array data repository. *Nucleic Acids Res.* 2002;30,207-210.

528 42. Robinson MD, McCarthy DJ, Smyth GK. edgeR: a Bioconductor package for
529 differential expression analysis of digital gene expression data. *Bioinformatics.* 2010;
530 26:139-140.

531 43. Maere S, Heymans K, Kuiper M. BiNGO: a Cytoscape plugin to assess
532 overrepresentation of Gene Ontology categories in Biological Networks.
533 *Bioinformatics.* 2005;21:3448-3449.

534 44. Shannon P, Markiel A, Ozier O, et al. Cytoscape: A Software Environment for
535 Integrated Models of Biomolecular Interaction Networks. *Genome Res.*
536 2003;13:2498-2504.

537 45. Szklarczyk D, Franceschini A, Wyder S, et al. STRING v10: protein–protein
538 interaction networks, integrated over the tree of life. *Nucleic Acids Res.*
539 2015;43:D447-452.

540 46. Eftang LL, Esbensen Y, Tannæs TM, Bukholm IR, Bukholm G. Interleukin-8 is the
541 single most up-regulated gene in whole genome profiling of H. pylori exposed gastric
542 epithelial cells. *BMC Microbiol*. 2012;12:9.

543 47. Jiang H, Zhou Y, Liao Q, Ouyang H. *Helicobacter pylori* infection promotes the
544 invasion and metastasis of gastric cancer through increasing the expression of matrix
545 metalloproteinase-1 and matrix metalloproteinase-10. *Exp Ther Med.* 2014;8:769-774.

546 48. Hewitt KJ, Agarwal R, Morin PJ. The claudin gene family: expression in normal and
547 neoplastic tissues. *BMC Cancer*. 2006;6:186.

548 49. Singh AB, Dhawan P. Claudins and cancer: Fall of the soldiers entrusted to protect
549 the gate and keep the barrier intact. *Semin Cell Dev Biol*. 2015;42:58-65.

550 50. Nishiguchi Y, Fujiwara-Tani R, Sasaki T, et al. Targeting claudin-4 enhances CDDP-
551 chemosensitivity in gastric cancer. *Oncotarget*, 2019;10:2189-2202.

552 51. Wroblewski LE, Shen L, Ogden S, et al. *Helicobacter pylori* dysregulation of gastric
553 epithelial tight junctions by urease-mediated myosin II activation. *Gastroenterology*.
554 2009;136:236-246.

555 52. Zhang C, Zhang H, Yu L, Cao Y. *Helicobacter pylori* dwelling on the apical surface
556 of gastrointestinal epithelium damages the mucosal barrier through direct contact.
557 *Helicobacter*. 2014;19:330-342.

558 53. Wroblewski LE, Piazuelo MB, Chaturvedi R, et al. *Helicobacter pylori* targets
559 cancer-associated apical-junctional constituents in gastroids and gastric epithelial
560 cells. *Gut*. 2015;64:720-730.

561 54. Romano M, Ricci V, Di Popolo A, et al. Helicobacter pylori upregulates expression of
562 epidermal growth factor-related peptides, but inhibits their proliferative effect in
563 MKN 28 gastric mucosal cells. J Clin Invest. 1998;101:1604-1613.

564 55. González-Mariscal L, Tapia R, Chamorro D. Crosstalk of tight junction components
565 with signaling pathways. *Biochim Biophy Acta*. 2008;1778:729-756.

566 56. Ding SZ, Smith MF, Goldberg JB. *Helicobacter pylori* and mitogen-activated protein
567 kinases regulate the cell cycle, proliferation and apoptosis in gastric epithelial cells. *J*
568 *Gastroenterol Hepatol*. 2008;23:e67-e78.

569

570 Figure Legends

571 Fig.1 Cell-cell tight junction disruption and delocalization of claudin-4.

572 MKN28 cells were infected with *H. pylori* 88-3887 for 24 hours. (A) Left panel shows
573 Epithelial barrier function of *H. pylori*-infected polarized MKN28 cells as analyzed by
574 measuring Trans-epithelial electrical resistance (TEER). Uninfected cells served as control.
575 Y-axis represents % baseline resistance calculated as described in the experimental methods
576 section. Right panel shows FITC-Dextran permeability values of *H. pylori*-infected MKN28

577 cells. Uninfected cells served as control. Y-axis represents the relative fluorescence units.
578 *indicates p-value<0.05. (B) Confocal micrographs of 24 hr *H. pylori*-infected MKN28 cells
579 showing delocalization of claudin-4 from the tight junctions as indicated by the white arrows
580 (Lower panel). 3-dimensional (3D) reconstruction of images was performed using Imaris
581 version 7.6. Uninfected cells served as control. Blue, DAPI-stained nuclei; Red, Cy3-stained
582 claudin-4; Green, Alexaflour 488- stained *H. pylori*. (C) Western blots of membrane and
583 cytoplasmic protein fractions of *H. pylori*-infected and uninfected MKN28 cells indicating
584 localization of claudin-4. P-cadherin and beta-tubulin served as controls for membrane
585 (Mem) and cytoplasmic (Cyto) fractions, respectively (upper panel). Western blots of
586 cytoplasmic and nuclear protein fractions of *H. pylori*-infected and uninfected cells indicating
587 localization of claudin-4 (lower panel). Beta-tubulin and Lamin A/C served as controls for
588 cytoplasmic and nuclear fractions, respectively. The image is representative of 3 independent
589 experiments. (D). Total protein lysate from *H. pylori*-infected and uninfected MKN28 cells at
590 indicated time points were immunoblotted using claudin-4 antibody. β-actin serves as loading
591 control for the experiment. The image is representative of 3 independent experiments (left
592 panel). Total mRNA from *H. pylori*-infected and uninfected cells were analysed for claudin-4
593 gene expression using qPCR. The experiment was done in triplicate and the relative
594 quantitation are expressed as histobars (right panel). GAPDH served as the endogenous
595 control for the experiment. UN: uninfected; WT: *H. pylori*-infected.

596 Fig.2 Effect of pretreatment with ERK activation inhibitor, U0126, on *H. pylori*-infected
597 MKN28 cells. (A) Epithelial barrier function of *H. pylori*-infected cells with and without
598 U0126 treatment was analyzed by measuring Trans-epithelial electrical resistance (TEER).
599 Y-axis represents % baseline resistance calculated as described in the experimental methods
600 section (left panel). FITC-Dextran permeability values of *H. pylori*-infected cells with and
601 without U0126 (MEK-inhibitor) treatment were determined. *indicates p-value<0.05. Y-axis

represents the relative fluorescence units (right panel). Uninfected cells with and without inhibitor served as controls. UN: uninfected, WT: wild-type *H. pylori*-infected. (B) Confocal micrographs of *H. pylori*-infected MKN28 cells with and without U0126 treatment showing localization of claudin-4. Blue, DAPI-stained nuclei; Red, Cy3-stained claudin-4. (C). Western blots of membrane and cytoplasmic protein fractions of *H. pylori*-infected cells with or without U0126 treatment indicating localization of claudin-4. (upper panel) P-cadherin and beta-tubulin served as internal controls for membrane and cytoplasmic fractions, respectively. Western blots of cytoplasmic and nuclear protein fractions of U0126 treated *H. pylori*-infected cells indicating the localization of claudin-4 (lower panel). Uninfected cells with and without inhibitor treatment served as controls. Beta-tubulin and Lamin A/C served as controls for cytoplasmic and nuclear fractions, respectively. Uninfected cells with and without inhibitor served as controls. UN: uninfected cells, WT: wild-type *H. pylori*-cells.

Fig.3 (A) Stacked column showing the number of significantly upregulated and downregulated genes in *H. pylori*-infected primary gastric cells. X-axis represents number of genes. (B) Scatter plot reveals the transcriptomic changes induced in *H. pylori*- infected cells. Grey dots represent genes that are not regulated by *H. pylori* whereas the blue dots represents the genes which are significantly altered in response to *H. pylori* infection. Representative dots of significantly upregulated genes are labelled on the plot. X-axis indicates the log10(RPKM) of the genes in uninfected cells (un) and Y-axis indicates the log10(RPKM) of the genes in *H. pylori*-infected cells (WT). (C) Heatmap demonstrating the RPKM values of the significantly regulated genes across replicates. The color scale depicts the log10(RPKM) starting from dark blue (lowest) to dark red (highest). The box to the left side presents examples of genes upregulated in *H. pylori*-infected cells and belonging to the indicated biological processes.UN1:Uninfected 1; UN2: Uninfected 2; WT1: *H. pylori*-infected 1; WT2: *H. pylori*-infected 2. (D) Gene Ontology analysis of genes upregulated in *H. pylori*-

627 infected cells denotes the enrichment of the indicated biological processes terms. The cell
628 junction and MAPK cascade associated GO terms are highlighted. X-axis is the – log10(p-
629 value) of the enriched GO term. (E) Interactions among proteins that are upregulated in *H.*
630 *pylori*-infected cells and associated with cell junction assembly and MAPK cascade are
631 visualized using Cytoscape 3.2.0. The violet nodes depict the MAPK cascade associated
632 genes and Orange nodes depict the cell junction assembly related genes.

A

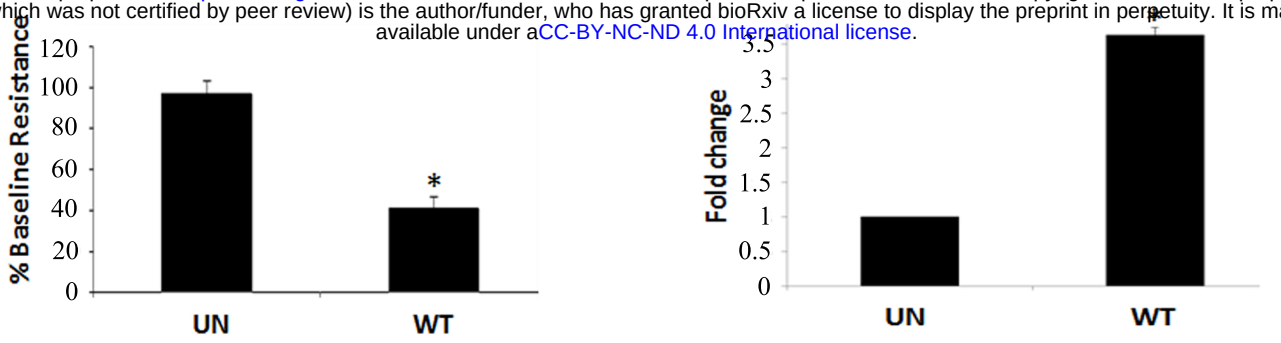

B

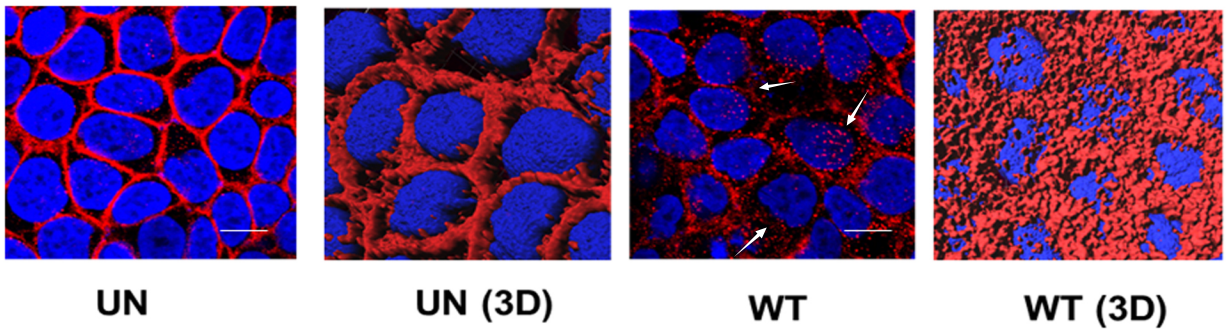

C

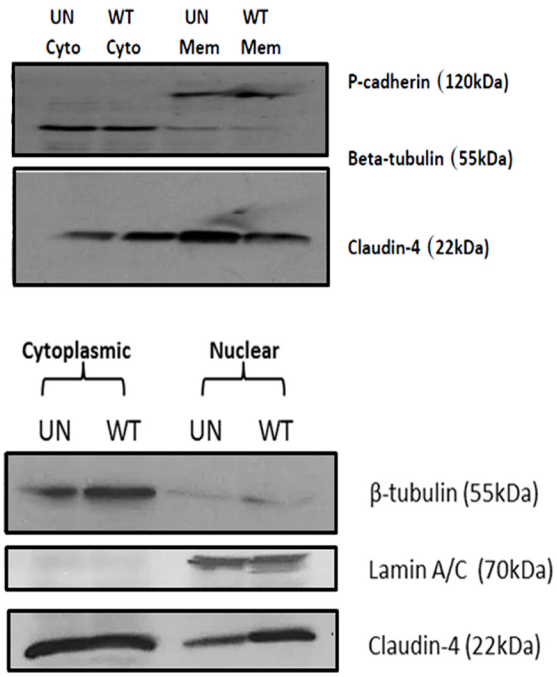

D

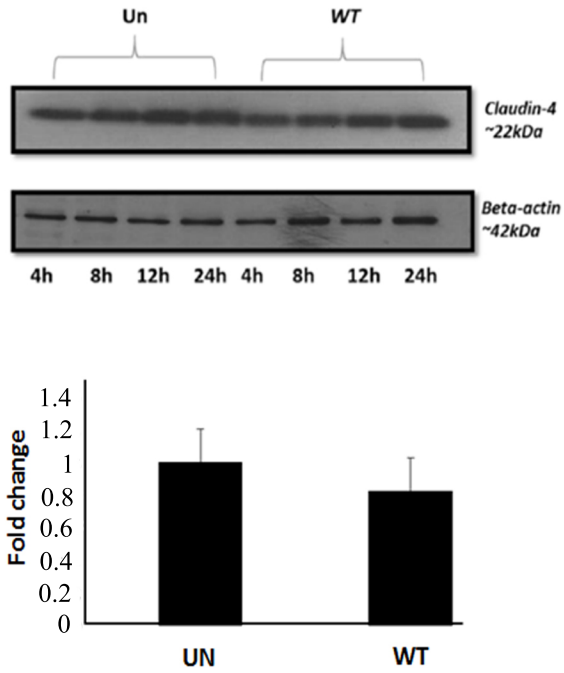

Figure 1

A

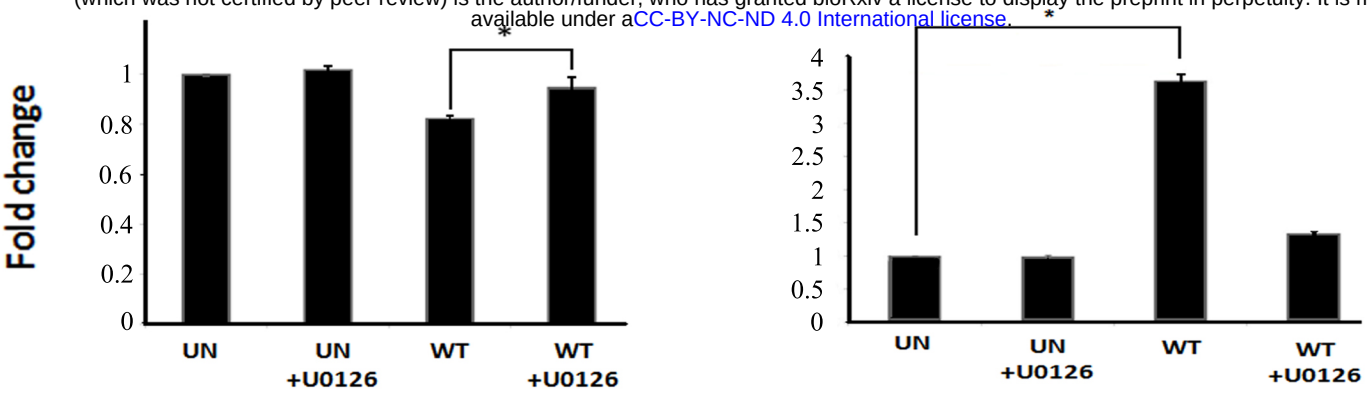

B

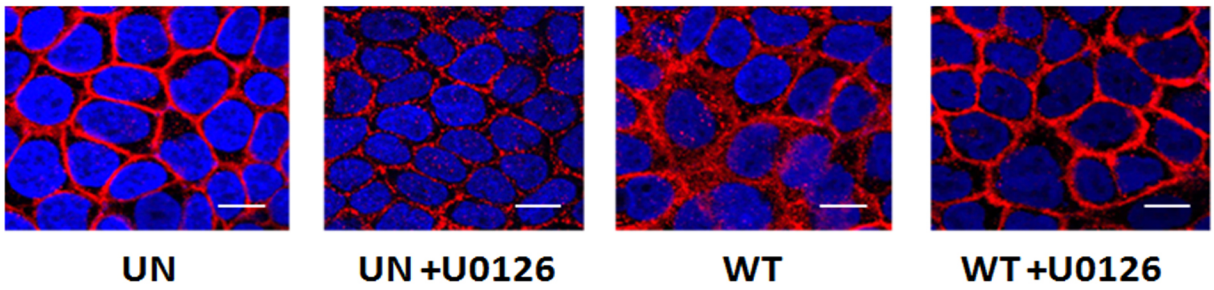

C

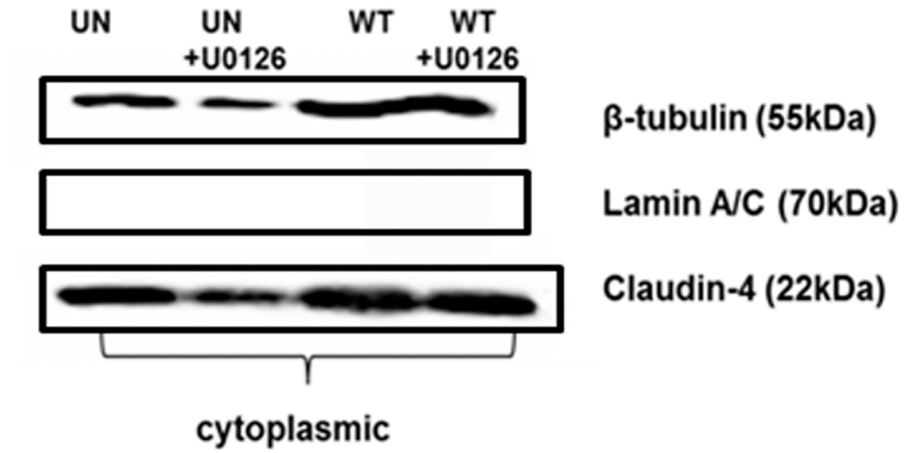

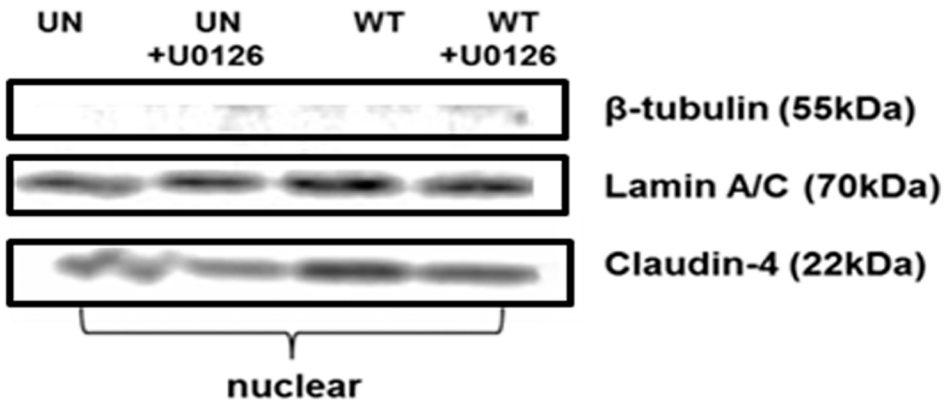

Figure 2

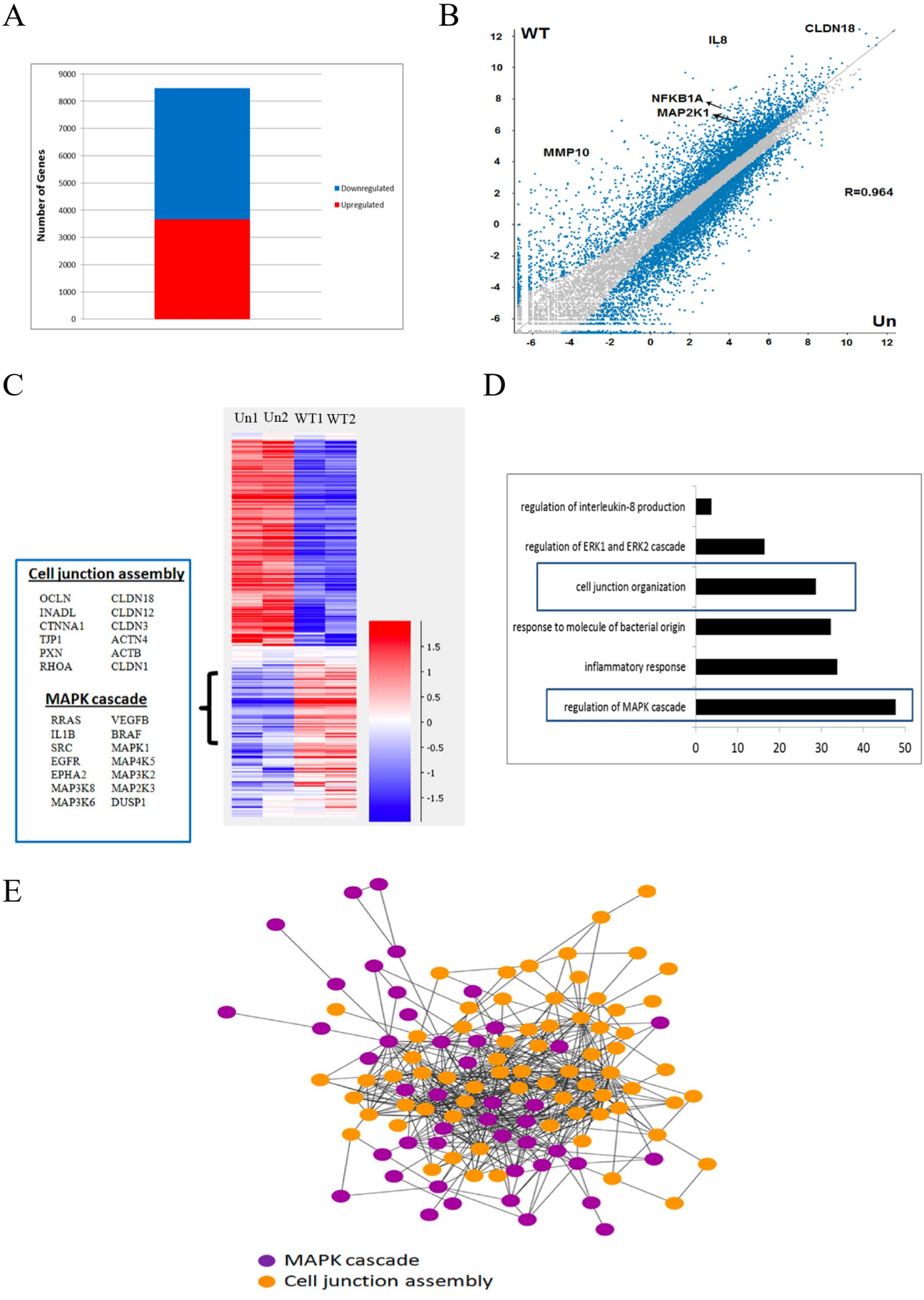
A
Number of Genes
9000
8000
7000
6000
5000
4000
3000
2000
1000
0
Downregulated
Upregulated
B
WT
IL8
CLDN18
NFKB1A
MAP2K1
MMP10
R=0.964
Un
12
10
8
6
4
2
0
-2
-4
-6
C
Un1 Un2 WT1 WT2
Cell junction assembly
OCLN
INADL
CTNNA1
TJP1
PXN
RHOA
CLDN18
CLDN12
CLDN3
ACTN4
ACTB
CLDN1
MAPK cascade
RRAS
IL1B
SRC
EGFR
EPHA2
MAP3K8
MAP3K6
VEGFB
BRAF
MAPK1
MAP4K5
MAP3K2
MAP2K3
DUSP1
1.5
1
0.5
0
-0.5
-1
-1.5
D
regulation of interleukin-8 production
regulation of ERK1 and ERK2 cascade
cell junction organization
response to molecule of bacterial origin
inflammatory response
regulation of MAPK cascade
0
10
20
30
40
50
E
MAPK cascade
Cell junction assembly

Figure 3